AIAA Modeling and Simulation Technologies Conference and Exhibit
11-14 August 2003, Austin, Texas

AIAA 2003-5676

The Results of a Simulator Study to Determine the Effects on Pilot Performance of Two Different Motion Cueing Algorithms and Various Delays, Compensated and Uncompensated

Liwen Guo*
Frank M. Cardullo†
Robert J. Telban‡
State University of New York
Binghamton, New York
Jacob A. Houck§
NASA Langley Research Center
Hampton, VA
Lon C. Kelly**
Unisys Corp.
Hampton, VA

Abstract

A study was conducted employing the Visual Motion Simulator (VMS) at the NASA Langley Research Center, Hampton, Virginia. This study compared two motion cueing algorithms, the NASA adaptive algorithm and a new optimal control based algorithm. Also, the study included the effects of transport delays and the compensation thereof. The delay compensation algorithm employed is one developed by Richard McFarland at NASA Ames Research Center. This paper reports on the analyses of the results of analyzing the experimental data collected from preliminary simulation tests. This series of tests was conducted to evaluate the protocols and the methodology of data analysis in preparation for more comprehensive tests which will be conducted during the spring of 2003. Therefore only three pilots were used. Nevertheless some useful results were obtained.

The experimental conditions involved three maneuvers; a straight-in approach with a rotating wind vector, an offset approach with turbulence and gust, and a takeoff with and without an engine failure shortly after liftoff. For each of the maneuvers the two motion conditions were combined with four delay conditions (0, 50, 100 & 200ms), with and without compensation.

Discrete time domain data of different variables were recorded and the Cooper-Harper Ratings (CHR) of simulator handling qualities were logged from the debriefing of the pilots who "flew" the simulator for the experiments. These two categories of data, allow both objective and quasi-objective evaluation, of the human controllers' performance. Power Spectral Density (PSD), an approach in the frequency domain was adopted for the analysis of the objective data. The PSD of the operator control behavior is an excellent indicator of operator workload. Among the analyses employing the PSD are the integral of the PSD over selected intervals and the analysis determining the frequency at which the peaks of the PSD occur.

From the analyses of the power spectral density, the total PSD of roll stick and pitch stick control in the 0 to 1 Hz range is slightly smaller when the optimal motion cueing algorithm is used in the straight-in approach and the offset approach. There is no noticeable difference of the total PSD of the pedal between the adaptive and the optimal motion cueing algorithms. When time delay is inserted, the total PSD of the roll stick, pitch stick and pedal control increases in the 0 to 1 Hz range, and increases significantly in the 0.17 to 0.4 Hz portion of the spectrum. Time delay also moves the highest peak of the PSD of the roll stick to a higher frequency area. Compensation reduces the total PSD, increased by the time delay, especially in the 0 to 0.4 Hz range. It also shifts the highest peak of PSD back to relatively lower frequencies. The paper will present details of the analysis including graphical representations of the results.

From the analyses of Cooper-Harper ratings, the optimal motion cueing algorithm shows better performance over the adaptive algorithm. The CHR does not increase when a time delay of up to 100 ms is presented. The mean CHR across all pilots in the straight-in approach and offset approach increases when compensation is applied, and the handling qualities rating becomes worse with compensation as delay increases. The compensation brings the mean CHR down only in the takeoff maneuver.

The paper describes the motion cueing algorithms used as well as the details of the manner in which the delays were inserted. The McFarland compensation algorithm will also be described.

* PhD Candidate, Department of Mechanical Engineering
† Associate Professor, Department of Mechanical Engineering, Associate Fellow AIAA
‡ PhD Candidate, Department of Mechanical Engineering, Student Member AIAA
§ Manager, Cockpit Motion Facility, Associate Fellow
** Software Engineer

Introduction

This paper reports on the analyses of the experimental data collected from the preliminary simulation tests, which were conducted on the Visual Motion Simulator (VMS), at the NASA Langley Research Center, in August, 2002. The preliminary experiments were designed to pave the way for the future formal simulations for investigating the effects of some transport delay compensation techniques and different motion cueing algorithms applied on a flight simulator. Discrete time domain data of different variables were recorded in ASCII format, and the Cooper-Harper Ratings of simulator handling qualities were also logged from the debriefing of the pilots involved in the study. These two categories of data serve as objective evaluation and subjective evaluation, respectively, and are the primary information employed to analyze the human controllers' performance. Power Spectral Density (PSD) analysis, an approach in the frequency domain, was adopted for the analysis of the objective data. The order of the paper is first, a brief description of the experimental conditions and the pilots. Then, it gives in detail the results of the analysis in terms of the integrated PSD in different intervals, regarding both motion cueing algorithm and the time delay compensation. Analysis based on peaks of the PSD plots is given followed by a comparison of the results from the PSD analysis and the Cooper-Harper rating. Finally, conclusions and recommendations for the future experiments complete the paper.

Visual Motion Simulator

The Visual Motion Simulator (VMS), shown in Figure 1, is a general-purpose simulator consisting of a two-crewmember cockpit mounted on a 60-inch stroke six-degree-of-freedom synergistic motion base[1,2]. Motion cues are provided in the simulator by the relative extension or retraction of the six hydraulic actuators of the motion base.

The cockpit of the VMS, shown in Figure 2, is designed to accommodate a generic transport aircraft configuration on the left side and a generic fighter or rotorcraft configuration on the right side. Both sides of the cockpit are outfitted with three heads-down CRT displays that present a generic electronic primary flight display, an electronic horizontal situation indicator display, and a generic electronic engine display; a number of small standard electromechanical circular instruments; and a gear handle mounted in the instrument panel. The left side contains a control loaded two-axis side stick, and the right side contains a control loaded two-axis center stick. Both sides contain control loaded rudder pedal systems. The center aisle stand is outfitted with a control display unit, a four-lever throttle quadrant, flap handle, speed brake handle, slats handle, etc. The cockpit is outfitted with four collimated window display systems to provide an out-the-window visual scene. The left side of the cockpit was used during this study.

Figure 1. The VMS simulator

The simulator includes a nonlinear mathematical model of a Boeing 757-200 aircraft, complete with landing gear dynamics, gust and wind models, flight management systems, and flight control computer systems. For this study, the test subjects flew the aircraft in the manual control mode (no autopilot) and with manual throttle control (no autothrottle).

Figure 2. The cockpit of the VMS simulator

The out-the-window visual scene is driven by an Evans and Sutherland ESIG 3000/GT computer generated image system. The visual database represented the Dallas/Fort Worth Airport and

surrounding terrain. The study utilized Runways 18L & 18R for approach cases and Runway 18R for takeoff cases. The runways were equipped with approach lights, precision approach path indicator lights, runway markings, and signage. The database included all runways and taxiways, and all airport structures and buildings. The study was conducted in a daylight environment with full visibility.

Test Conditions

The study consisted of four flight scenarios: (1) a straight-in approach, (2) an offset approach, (3) a normal takeoff, and (4) a takeoff with engine failure. The details of the flight scenarios are described below:

(1) Straight-in Approach

- Altitude - 1300 ft BARO, 697 ft AGL
- Airspeed - 135 kts
- Heading - 180 deg
- Distance to runway - 2 nm
- Flaps - Full, Gear - Down
- EPR - 1.19
- On Glideslope, On Localizer
- Wind Conditions - 10 kts, Begins as a head wind, swings around to a 90 deg wind from the left at 1 nm, and continues to swing around to a tail wind as the aircraft crosses the threshold.

Procedure –

Visual approach,
PAPI lights available on Runway 18R,
Glideslope and Localizer needles available on Primary Flight Display

(2) Offset Approach

- Altitude - 1300 ft BARO, 697 ft AGL
- Airspeed - 135 kts
- Heading - 180 deg, aligned with Runway 18L
- Distance to runway - 2 nm
- Flaps - Full, Gear - Down
- EPR - 1.19
- On Glideslope
- Wind Conditions - Severe Turbulence. Lateral gust from the left, 90 deg to runway centerline, turns on at 3000 ft from runway threshold, turns off at the runway threshold.

Procedure –

When the red light on instrument panel illuminates (7500 ft from threshold), realign approach and land on Runway 18R,
Visual approach, PAPI lights available on Runway 18R,
Glideslope and Localizer needles available on Primary Flight Display

(3) Takeoff - With or without engine failure

- Runway 18R
- Flaps - 15 deg
- Takeoff EPR - 1.60
- V_R - 126 kts
- For engine failure cases, left engine failure at 1300 ft BARO, 697 ft AGL

Procedure -

Apply brakes
Advance throttles from idle to Takeoff EPR
Release brakes
At V_R, rotate to 15 deg pitch-up attitude
Climb to 2000 ft BARO while accelerating to 200 kts
Retract gear and flaps as appropriate
Maintain runway heading of 180 deg during takeoff

Three pilots took part in the 168 preliminary cases, each accounting for 56 test runs in a single day. One is a NASA simulator pilot, one is a NASA test pilot who flies the Boeing 757 airplane for the Langley Research Center, and one is a NASA engineer certified to fly Boeing 757 airplanes. The 56 test runs fall into three groups based on the three maneuvers—16 for the Straight-in approach (SA), 16 for the Offset approach (OA) and 24 for the Taking Off (TO). In an offset approach, the aircraft is initially lined up with the left runway, then it offsets to the parallel runway on the right within a certain distance of transition. Turbulence was added in the offset approach. The 16 runs for the first two maneuvers come from the enumeration of combinations of three simulation conditions—four different time delays, 0, 50, 100 & 200ms; two motion cueing algorithms, the Adaptive algorithm and the Optimal algorithm, and with or without compensation, account for $4 \times 2 \times 2 = 16$ cases. For the takeoff maneuver, there are eight more cases because one more condition was added, that is, with/out the engine failure. The order of all cases in each maneuver group was made random, the zero delay case is not necessarily the first run, and an uncompensated case is not necessarily followed by a compensated case. The 56 randomized cases are listed in Tables 1 and 2.

Two motion cueing algorithms were implemented for the experiments on the NASA Langley Visual Motion Simulator (VMS). The first technique is the coordinated adaptive washout algorithm, or "adaptive algorithm" developed at NASA[3]. The objective of this

algorithm is to adjust the cueing algorithm gains based upon its current motion states by minimizing a cost function in real time. The second technique is a revised "optimal algorithm" developed by Telban, et al.[4] that is based on the concept first proposed by Sivan, et al.[5]. This algorithm uses higher-order linear filters that are developed using optimal control methods that incorporate new mathematical models of the human vestibular system.

①	②	③	④	⑤	①	②	③	④	⑤
STRAIGHT IN APPROACH	1	0	0	1	OFFSET APPROACH	17	0	0	0
	2	100	1	0		18	0	1	0
	3	0	1	1		19	200	1	1
	4	50	0	1		20	50	0	0
	5	0	1	0		21	100	0	1
	6	100	0	0		22	50	1	0
	7	0	0	0		23	0	0	1
	8	100	0	1		24	200	0	1
	9	50	1	0		25	100	1	1
	10	200	1	0		26	50	0	1
	11	100	1	1		27	200	0	0
	12	50	1	1		28	50	1	1
	13	200	1	1		29	0	1	1
	14	200	0	0		30	100	0	0
	15	50	0	0		31	100	1	0
	16	200	0	1		32	200	1	0

Table 1. Test runs and conditions

①: Maneuver; ②: Test run order; ③: Time delay (millisecond); ④: Motion cueing algorithm, with "0" for Adaptive and "1" for Optimal; ⑤: Compensation, "0"—without and "1"—with.

The McFarland algorithm was employed to compensate for the delays in the preliminary experiments. The McFarland compensator, a special integrator, uses the previous two steps of velocity to extrapolate or predict the compensated displacement, or mathematically, it is given by

$$u_c(k) = u_d(k) + b_0 v_d(k) + b_1 v_d(k-1) + b_2 v_d(k-2) \qquad (1)$$

where u stands for the displacement, v the velocity, subscript c the compensated and subscript d the delayed. Coefficients b_0, b_1 and b_2 are determined by tuning the sinusoidal input signal[6,7].

In each test run, about 60 variables were sampled and recorded. The sampling period is 16 ms and one out of four samples was recorded, indicating a decimation ratio of 4 and the decimated period of 64 ms. About 1000 data points were collected for each variable.

TAKE OFF										
①	②	③	④	⑤		①	②	③	④	⑤
33	0	0	1	1		45	0	0	0	0
34	0	1	1	0		46	100	1	1	1
35	200	1	0	1		47	200	0	1	0
36	50	0	0	1		48	100	0	0	0
37	50	0	1	0		49	100	1	0	1
38	200	1	1	1		50	50	0	0	1
39	50	1	0	0		51	0	1	1	1
40	100	0	1	0		52	50	0	0	1
41	50	1	1	1		53	100	0	1	1
42	0	1	0	1		54	200	1	1	0
43	200	0	0	1		55	0	1	1	1
44	100	1	0	1		56	200	1	1	1

Table 2. Test runs and conditions

①: Test run order; ②: Time delay (millisecond); ③: Motion cueing algorithm, with "0" for Adaptive and "1" for Optimal; ④: Compensation, "0"—without and "1"—with; ⑤: Engine failure: "0"—without and "1"—with.

Data collection

The test runs were recorded using DVD and videotape. The images recorded were (1) camera pointed at back of motion system, (2) camera pointed at side of motion system, (3) pilot's out-the-window display, and (4) pilot's primary flight display (EADI). Pilot comments during and after test runs were recorded along with a Cooper - Harper Rating for the run.

Analysis of the total PSD within certain intervals

Among the 60 variables recorded, the analysis was carried out primarily on the four control inputs of the pilot, the roll stick, pitch stick, rudder pedals and the

throttle, which are directly related to the operator's control performance. Since the analysis shows that the change of simulation conditions, such as changing the amount of delay or motion cueing algorithm, only makes a trivial difference on the throttle control, only the roll stick, pitch stick and pedal controls were analyzed.

The power spectrum or power spectral density of a discrete process is the discrete time Fourier transform (DFT) of its autocorrelation sequence[8,9]. In mathematical terms, the PSD is proportional to the square of the magnitude of the process; hence it is closely related to the energy of the signal as a function of the frequency. Therefore, the total PSD, or the integration of PSD over a certain range of frequencies of the control variable reveals the energy the human operator exerts on the control, thereby providing some insight into the pilot's control performance. Usually higher PSD means poorer handling qualities and therefore higher pilot workload. One drawback of the PSD analysis is the loss of phase information.

There are over 10 different methods to calculate the PSD of a signal, and two of them are used for the PSD calculation in this paper, the direct method and the indirect method. The direct method, namely, the periodogram, is a synonym for the square magnitude of the DFT. The periodogram shows all details of the PSD. On the other hand, the indirect method, or the smoothed periodogram, is the DFT of the autocorrelation, in other words, the autocorrelation must be calculated first. The smoothed periodogram suppresses some random details of the PSD so as to show the microscopic characteristics of it. For smooth signals, the periodogram will be used for examining the peak details, while for signals with more noise, such as the control activity, the smoothed periodogram will be used to eliminate the artifacts of noise.

The average of a signal is deducted from it before calculating the PSD to avoid an artificial peak at zero Hz, which may dominate the PSD and make other meaningful peaks invisible. Zero pad is also applied to increase the resolution of the adjacent peaks. After investigation, the Hamming Window Method is adopted for the calculation of PSD.

For most of the 168 cases, the PSD of a control input, outside the interval [0 1] Hz contributes less than 5% to the total PSD, and because of that, the PSD over the range [0 1] Hz of a control input is a reasonable measure of the total energy the pilot uses for control. In this sense, the cutoff frequency of control may be taken as 1 Hz. But the pedal control has a narrower band, with a cutoff frequency 0.6 Hz. For the purpose of simplicity, bar charts, as shown in the lower part of Figure 3, are used to compare the total PSD of different tests. In Figure 3, the height of a bar equals the area of the region formed by the corresponding PSD curve, the X-axis and the interval. Euler integration was used to calculate the area.

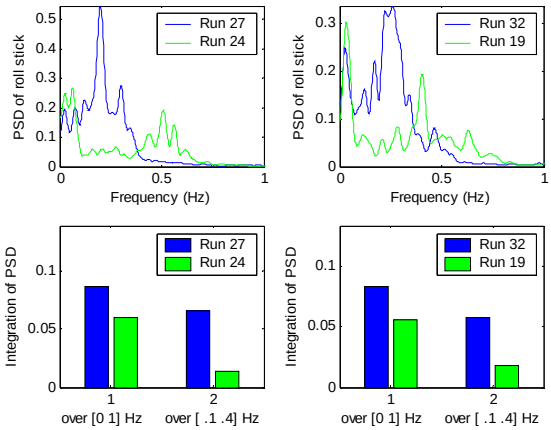

Figure 3. An example of the PSD curves and their bar charts

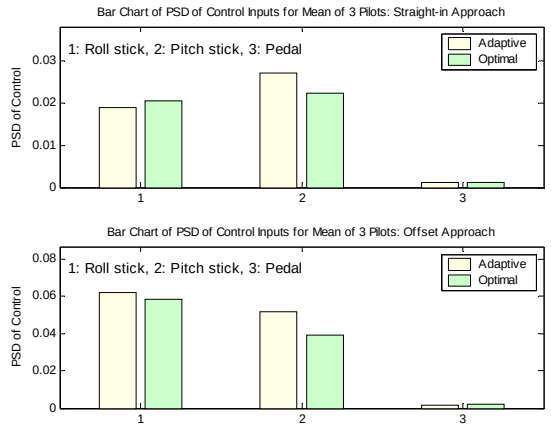

Figure 4. Bar charts of average PSD for comparing the motion algorithms

Motion Cueing Algorithms

To eliminate possible effects of time delay or compensation, only the zero delay cases were selected for the comparison of the motion cueing algorithms. Figure 4 shows the bar charts of average total PSD of control inputs across the three pilots for the straight-in approach and the offset approach. The average of the total PSD of the optimal cueing algorithm tends to be slightly lower than that of the adaptive cueing algorithm for the roll stick and pitch stick control. However,

exceptions exist; for example, the average PSD of roll stick control for the straight-in approach is higher with the optimal cueing algorithm than with the adaptive algorithm. In addition, there is no noticeable difference associated with the motion cueing algorithms for the pedal control. This may be a consequence of the fact that the PSD of pedals is very small compared with that of the roll and pitch stick control, showing that the pilot's workload increased very little as a result of pedal utilization. The takeoff cases fall into two groups, with or without engine failure. In the group of engine failure, there is only one test run of each motion cueing algorithm for each pilot, which may not be sufficient to yield any meaningful result. In the group of engine failure, the optimal motion cueing algorithm reduces the total PSD of both roll and pitch stick control, and the reduction is significant for the roll stick. For the pedal, the optimal motion cueing algorithm seems to be showing larger control PSD; however, as it will be stated in the part "Effect of Engine Failure", the engine failure increases the pedal PSD tremendously.

Effect of Time Delay

The bar charts in Figure 5 and 6 show the effect of the time delay. Apart from the pitch stick control of the offset approach, the PSD tends to increase as the time delay was added. For most cases, the longer the time delay, the higher the total PSD. There is a substantial increase of PSD of the roll stick control when 200 ms delay was inserted. Again, the PSD of pedal control is much smaller than the other two control inputs, and the time delay tends to bring some noticeable increase on the total PSD, but with some exceptions. Finally, it seems like the increase of PSD caused by the time delay is a little more obvious with the optimal motion cueing algorithm than with the adaptive one.

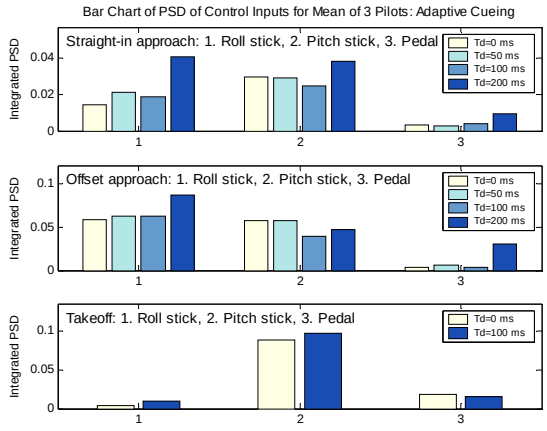

Figure 5. Bar charts of average PSD showing the effect of time delay: adaptive motion cueing

Middendorf, et al[10] has reported that power in the [0.4 0.5] Hz range significantly increased as the time delay increases, according to their research on the offset approach simulation tests. One thing to notice is in addition to the 90 ms baseline delay introduced by the aircraft dynamics, 200 ms or 300 ms transport delay was inserted between the pilot input and the pilot cueing by the visual display. This added delay is much larger in amount than the delay in our research. However, it offers a good point to investigate the effect of time delay on the PSD in some subintervals lying in [0 1] Hz range, and the result is summarized in Table 3. The intersection of the increasing ranges is [0.17 0.4] Hz, in other words, the PSD in this range was significantly increased by the time delay.

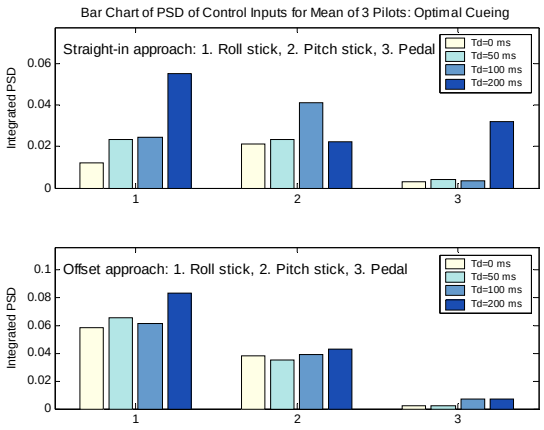

Figure 6. Bar charts of average PSD showing the effect of time delay: optimal motion cueing

Maneuver		Straight-in Approach (Hz)	Offset Approach (Hz)
Roll Stick	Adaptive	[0 .55]	[0 .40]
	Optimal	[0 .50]	[0 .40]
Pitch Stick	Adaptive	[0 .44]	[.15 .48]
	Optimal	[0 .40]	[.17 .57]
Pedal	Adaptive	[0 .52]	[0 .40]
	Optimal	[0 .65]	[0 .40]

Table 3. Frequency ranges in which the PSD increased obviously by the delay

Effect of Compensation

Figure 7, 8 and 9 are the bar charts of the total PSD of control inputs in [0 1] Hz for those tests with the

McFarland delay compensation algorithm. In general, tests with compensation have lower total PSD for the roll stick and pitch stick control, and the effect of compensation is more obvious when time delay is longer. Most exceptions take place for the pedal control of all straight-in approach and offset approach tests as well as some takeoff tests without engine failure. For all these cases, the PSD of the pedal is much smaller than the other two control inputs, which implies little or no pedal workload from the pilot, and the collected data of pedal might be artifacts or noise. Three exceptions for the roll and pitch stick control inputs, i.e., two for 100 ms delay and one for 200 ms delay (see Figure 8 and 9), share a common condition—adaptive motion cueing algorithm was used, possibly suggesting better compensation effects from the use of optimal motion cueing algorithm.

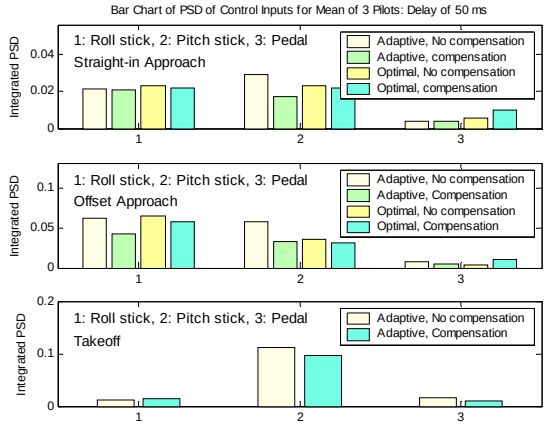

Figure 7. Bar charts of average PSD showing the effect of delay compensation for a 50 ms delay

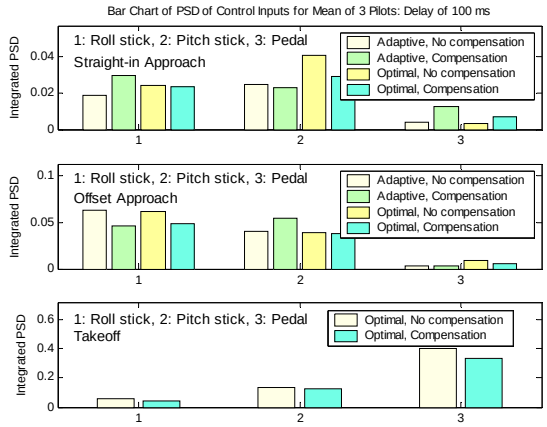

Figure 8. Bar charts of average PSD showing the effect of delay compensation for a 100 ms delay

Again, it is worth examining the PSD of some subintervals within [0 1] Hz. The range in which the PSD was decreased by the compensation for different cases is summarized in Table 4. A rough intersection of all those intervals is [0 0.4] Hz. In other words, the control quality of operators was substantially better in [0 0.4] Hz when McFarland compensation is applied. At frequencies of 0.4 Hz or above, the pilot showed even poorer control performance, especially for 200 ms delay compensation.

Maneuver		Straight-in Approach (Hz)	Offset Approach (Hz)
Roll Stick	50 ms	[.17 .5]	[0 .42]
	100 ms	[.2 .5]	[0 .45]
	200ms	[0 .43]	[0 .4]
Pitch Stick	50 ms	[0 .7]	[0 .7]
	100 ms	[0 .6]	[0 .6]
	200ms	[0 .38]	[0 .5]
Pedal	50 ms	[.17 .6]	[.2 .42]
	100 ms	[0 .22]	[0 .4]
	200ms	[0 .34]	[0 .4]

Table 4. Frequency ranges in which the PSD decreased obviously by compensation

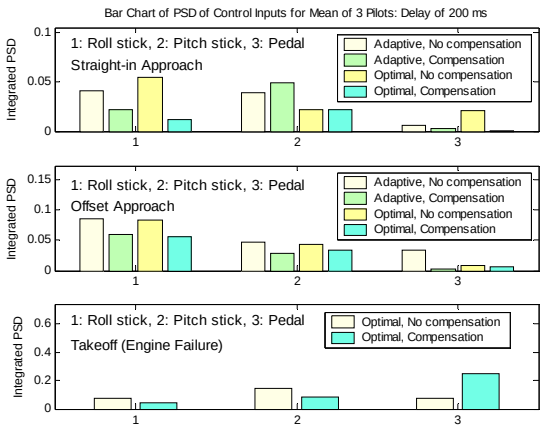

Figure 9. Bar charts of average PSD showing the effect of delay compensation for a 200 ms delay

The poorer control performance above 0.4 Hz when the McFarland compensation was used may come from the design nature of the McFarland filter itself. First, it displays large gain distortion when the operating frequency exceeds 3 Hz—the cutoff

frequency. Secondly, the three coefficients of the filter were determined by employing sinusoidal signal tuning. When a non-sinusoidal signal in the real world is presented, errors result even below the cutoff frequency. Figure 10 shows the Bode diagram and step response of a system with a McFarland filter applied on a 4th order aircraft dynamics model and a human operator model when 200 ms artificial time delay was added. The Bode diagram on the left shows apparent gain distortion above 12 rad/s and the lack of phase lag compensation. The unit step responses are shown on the right, with the bottom graph the zoom of the top one. Because of the infinite acceleration resulting from the step input the response oscillates at a high frequency until it subsides, and follows the non-delayed response.

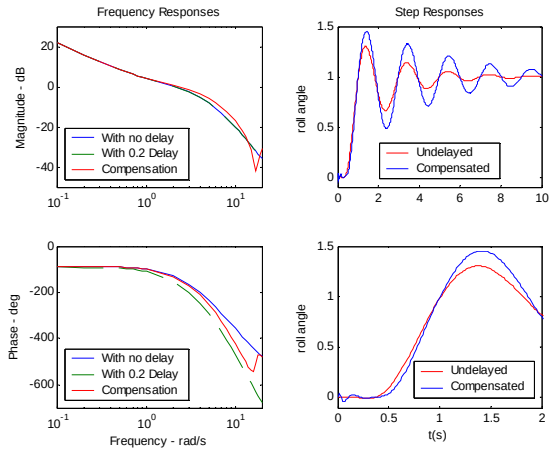

Figure 10. Responses of a control system with the McFarland filter

Effect of Engine Failure

The effects of engine failure on the PSD of control operation of the pilot in the takeoff maneuver are illustrated in Figure 11; the top graph is for the adaptive motion cueing algorithm and bottom for the optimal. There are two obvious effects caused by the engine failure. First, the engine failure always increases the total PSD of each control, the roll and pitch stick and the rudder pedal. Second, it increases the pedal PSD tremendously, and the increase is so large that it dominates the effect of the four factors—the time delay, compensation, motion cueing algorithm and the engine failure.

Analysis on the Peaks of the PSD

Figure 12 shows the time domain plots of the roll angle and roll stick activity of two test runs of the offset approach maneuver. Starting at the 20th second, the aircraft rolls to the right and eventually the glide slope is acquired at about the 64th second, indicating the entire offset approach maneuver takes about 44 seconds.

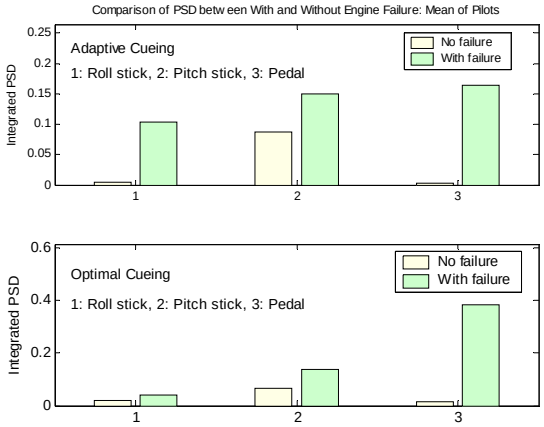

Figure 11. Bar charts of total PSD of tests of takeoff with or without engine failure

The roll stick and roll angle are the input and output of a control system with the aerodynamics serving as a filter, and the filtering makes the roll angle plot much smoother. For this reason, the PSD of the roll angle was calculated using the direct method—the periodogram. In addition, since only the peaks of PSD are of interest in this section, the PSD of roll angle was normalized. But for consistency with other sections, the PSD of the roll stick was still calculated with the indirect method—the smoothed periodogram. The PSD plots of the roll angle and roll stick activity of the same two test runs are given in Figure 13.

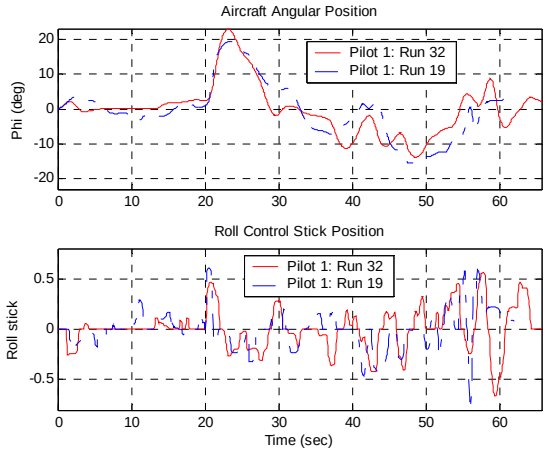

Figure 12. Roll angle and roll stick activity of two tests of offset approach

For the offset approach, the highest peak PSD is always the first peak, and is located at 0.0029 Hz, the inverse of which is close enough to 44 seconds—the duration of the offset maneuver, that it is reasonable to relate this peak to the offset approach. This relation is also mentioned in the paper of Middendorf, et al. The dominant peak of the straight-in approach and takeoff are not located at 0.0029 Hz. The PSD of the roll angle of most offset approach test runs has a second peak located at about 0.06 Hz. Unlike the dominant peak, this peak is not present for all offset approach runs. Because the PSD of the roll angle of the straight-in approach and takeoff does not have such a peak at 0.06 Hz, this peak may also be related to the offset approach maneuver. One thing worthy of clarifying is in the paper of Middendorf, et al, these two peaks are stated to be of the control activity, however they are actually of the roll angle. The PSD of the roll stick control activity, as shown in the bottom graph in Figure 13, has many more peaks, even after it was smoothed.

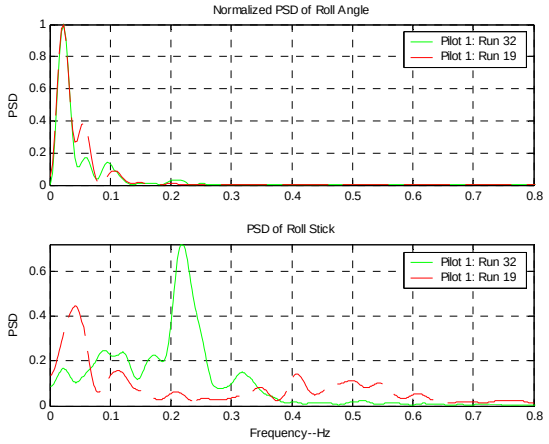

Figure 13. PSD of the roll angle and roll stick activity of two tests of offset approach

For both the straight-in and offset approaches, when there is no time delay, the highest peak of the PSD of the roll stick or the pitch stick is either the first peak, or near the first peak. When time delay is presented, the highest peak tends to move to the right, or higher frequency area, but the compensation moves it back to low frequencies (Figure 14). In other words, time delay increases the operator's workload in the high frequencies but the compensation decreases it. That is similar to the result from the analysis on the total PSD.

For all maneuvers, the motion cueing algorithms make no obvious difference to the peaks of the PSD, except that the McFarland filter seems to achieve better compensation effect when the optimal algorithm is used.

Analysis of the Cooper-Harper Ratings

The Cooper-Harper rating (CHR)[11] is one way to judge aircraft handling qualities. It is a subjective evaluation because the test pilots are required to make a series of decisions concerning the difficulty of controlling the aircraft. The Cooper-Harper rating is an overall evaluation instead of reflecting a single factor such as the responsiveness; hence two simulations with a close Cooper-Harper rating may have quite different dynamic responses. For these two reasons, a Cooper-Harper rating may give rise to conflicting results with respect to other analysis techniques, such as the PSD analysis. Higher CHR means poorer handling quality. Of the 10 values of the Cooper-Harper scale, ratings of 1, 2 and 3 fall in level I, ratings of 4, 5 and 6, in level II, and ratings of 7, 8, 9 and 10, in level III. Jumping from one level to another is said to be a significant change of handling qualities.

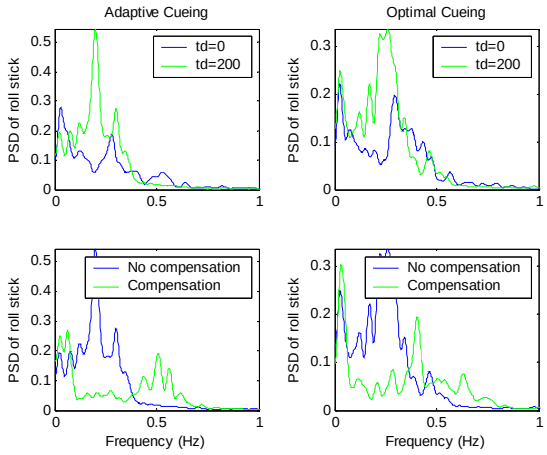

Figure 14. Movement of the highest peak of the mean PSD of the roll stick caused by the time delay and the compensation.

Figure 15 illustrates the difference of mean values and the standard deviations of the Cooper-Harper rating caused by different motion cueing algorithms, averaged across all maneuvers. All three pilots reported obvious better handling qualities when the optimal motion cueing algorithm was used, and pilot 3 even displayed significant change of CHR. However, it does not agree with the result from the PSD analyses, which shows no apparent difference between the two motion cueing algorithms. Finally, including the engine failure in the takeoff maneuver makes no noticeable difference to the average Cooper-Harper rating of the two motion cueing algorithms.

The Cooper-Harper rating also produces controversial results compared to those from the PSD analyses with regard to the effects of time delay and compensation. The mean values and standard deviations of the CHR across all pilots and maneuvers are shown in Figure 16. Notice that it makes no sense to have compensation for the zero delay, so the two cases of zero delay are actually the same and may be merged together to calculate the average. The mean CHR even decreases when a time delay of 50 ms or 100 ms is introduced without compensation, and for a delay of 200 ms it increases so slightly that it is hardly noticeable. It shows that, in terms of CHR, a delay up to 100 ms is not perceivable for the pilots, or it might be perceivable but it they did not reveal the effect of delay to their CHR, which demonstrates the subjective property of the CHR. For the 50 ms and 100 ms delay cases, no obvious decrease of the mean CHR caused by the compensation is shown when averaged across all maneuvers, the average CHR is even higher with the compensation in straight-in approach and offset approach, and only in the takeoff the mean CHR decreases considerably with compensation. For all maneuvers, the CHR increases obviously when compensation is used for a delay of 200 ms. For this case (200 ms delay with compensation), pilot 2 and 3 gave some test runs CHR values of 10, which may account for the obvious increase. These high ratings might have resulted from a motion system glitch or some other anomaly.

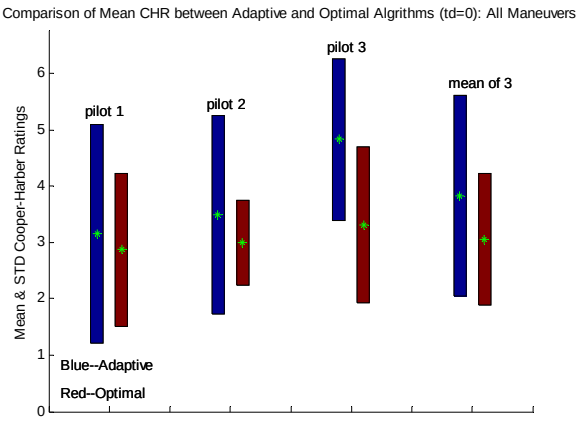

Figure 15. Bar Chart of mean and standard deviation of CHR for comparing motion cueing algorithms (The center vertical position of the bar indicates the mean value of the CHR and the length of the bar the standard deviation. Only zero delay runs are included.)

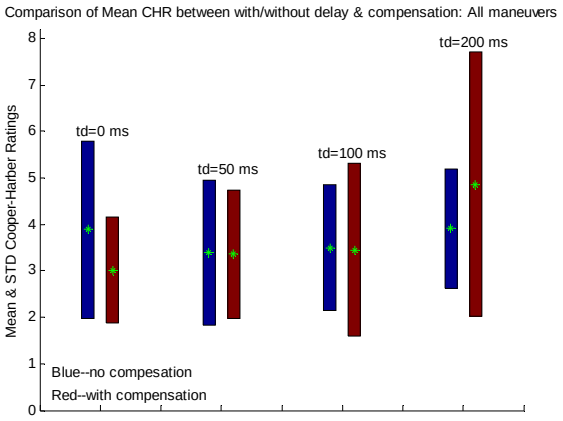

Figure 16. Bar Chart of mean and standard deviation of CHR Concerning time delay and compensation (The center vertical position of the bar stands for the mean value of CHR and the length of the bar the standard deviation. Only zero delay runs are included.)

Conclusions

1. From the analyses of the power spectral density, the total PSD of roll and pitch stick control in the [0 1] Hz range is slightly smaller when the optimal motion cueing algorithm is used in the straight-in approach and offset approach. No noticeable difference of the total PSD of the pedal between the adaptive and the optimal motion cueing algorithms is seen. When time delay is inserted, the total PSD of the roll stick, pitch stick and pedal control increases in the [0 1] Hz range, and increases significantly in the [0.17 0.4] Hz range. Time delay also moves the highest peak of the PSD of roll stick to a higher frequency area. Compensation obviously lowers the total PSD increased by the time delay, especially in the [0 0.4] Hz range. It also shifts the highest peak of PSD back to relatively lower frequencies. Engine failure in the takeoff maneuver dominates the effects of other experimental conditions such as motion cueing algorithm, time delay amount or compensation, and it increases the workload of rudder pedal significantly.

2. From the analyses of Cooper-Harper ratings, the optimal motion cueing algorithm shows better performance over the adaptive algorithm. The CHR does not increase when a time delay of up to 100 ms is presented. The mean CHR, across all pilots in the straight-in approach and offset approach, increases when compensation is applied, and the handling qualities become worse with compensation as delay increases. The compensation brings the mean CHR down only in the takeoff maneuver.

3. As for future research, the next phase of this study will include 11 pilots. A non-linear motion cueing algorithm, where the Riccati equation will be solved in real-time, will be employed. Finally, two additional compensation algorithms will be tested.

References

[1] Parrish, R. V., Dieudonne, J. E., Martin, D. J., Jr., and Copeland, J. L., "Compensation Based on Linearized Analysis for a Six-Degree-of-Freedom Motion Simulator," NASA TND-7349, 1973.

[2] Parrish, R. V., Dieudonne, J. E., and Martin, D. J., Jr., "Motion Software for a Synergistic Six-Degree-of-Freedom Motion Base," NASA TND-7350, 1973.

[3] Martin, D. J., Jr., "A Digital Program for Motion Washout on Langley's Six-degree-of-freedom Motion Simulator," NASA Langley Research Center, Contractor Report 145219, Hampton, VA, July 1977.

[4] Telban, R. J., Cardullo, F. M., and Houck, J. A., "Developments in Human Centered Cueing Algorithms for Control of Flight Simulator Motion Systems," *AIAA Modeling and Simulation Technologies Conference*, Portland. OR, 1999.

[5] Sivan, R., Ish-Shalom, J. and Huang J. K., "An Optimal Control Approach to the Design of Moving Flight Simulators," *IEEE Transactions on Systems, Man, and Cybernetics*, Vol. 12, No. 6, 1982, pp. 818-827

[6] McFarland R. E., CGI Delay Compensation, NASA Ames Research Center, 1986.

[7] McFarland R.E., Transport Delay Compensation for Computer-Generated Imagery Systems, NASA Ames Research Center, 1988.

[8] Porat B., A Course in Digital signal Processing, John Wiley & Sons, Inc, 1996.

[9] Hayes M. H., Statistical Digital Signal Processing and Modeling, John Wiley & Sons, Inc, 1996.

[10] Middendorf M. S., Lusk S. L., Power Spectral Analysis to Investigate the Effects of Simulator Time Delay on Flight Control Activity, Armstrong Aerospace Medical Research Laboratory, 1990.

[11] Cooper F. R., Harris W. T. and Sharkey V. J., Effects of Visual System Time Delay on Pilot Performance, Naval Training Equipment center, 1975.